

METAL-CERAMIC COMPOSITE LATTICE STRUCTURES USING 3D PRINTED SAND MOLDS AND CORES

A.P. Druschitz¹, S. Cowden¹, A. Dudley¹, S. Walsh¹, A. Weir¹, C.B. Williams², B. Wood³

¹Department of Materials Science and Engineering, Virginia Tech, Blacksburg, VA, 24061

²Department of Mechanical Engineering, Virginia Tech, Blacksburg, VA, 24061

³ExOne, North Huntingdon, PA 15642

Abstract

Binder Jetting of sand molds for metal casting provides a scalable and efficient means of fabricating large metal parts with complex geometric features made possible only by Additive Manufacturing. For example, in earlier work, the authors demonstrated the use of Binder Jetting to fabricate complex mold structures for casting large-scale, lightweight metallic lattice structures and sandwich panels that could not be made through either traditional sand casting or through other direct metal AM techniques. In this paper, the authors demonstrate the fabrication of metal-ceramic composite lattice structures via embedding ceramic tiles into the printed mold package. The addition of ceramic tiles can add resistance to penetrators and/or radiation shielding to the lightweight lattice structures, which can be tailored for energy absorbing performance. 3D printed mold and core designs for metal and metal-ceramic composite lattice castings are described along with 3D printed mold designs for encapsulating individual metal or ceramic tiles.

Keywords: metal casting, 3D printed sand, mesostructure, ceramics, composites, encapsulation

1. Multi-Functional Lattice Structures

1.1. Motivation

There is continued interest for lightweight ballistic armor that will improve vehicle performance and safety while also decreasing vehicle transportation costs. To address this challenge, and other challenges associated with lightweighting structures, many have looked to the design and fabrication of cellular materials. Cellular materials are low density, porous structures that provide excellent characteristics including high strength, high stiffness, and high energy absorption, while maintaining low mass [1–3]. Due to their unique combination of low mass and high stiffness, cellular materials have found application in automotive, aerospace, military, and infrastructure industries. The porosity has been used to realize advanced filters, heat exchangers, biomedical prostheses, and blast resistant panels [3,4]. A wide range of traditional manufacturing techniques have been employed to fabricate complex cellular structures, resulting in both stochastic (e.g., via gas foaming [5]) and ordered (e.g., via stamping and joining of metal sheets [6]) cellular material topologies.

While cellular materials, and sandwich panels in particular, have been shown to be effective in mitigating blast load while maintaining a minimum mass, they alone do not effectively meet all of the design requirements for armor applications. Instead, a multi-

functional material solution is needed that offers low-mass while also effectively offering protection from both blast impact and projectiles.

1.2. Metal Matrix Composites

To achieve this multi-functionality, metal matrix composite (MMC) armors have been traditionally used. MMCs feature two dissimilar materials: a metal matrix featuring an embedded constituent material, which is typically a ceramic [7]. The matrix material supports and transmits loads distributed to the encapsulated ceramic, which acts as a reinforcement to improve the matrix properties [8]. For example, a composite component formed by combining a material with a high toughness with another material of high hardness will have the characteristics of both materials (i.e., high toughness and hardness). Relative to their metal counterparts, MMCs have shown decreased density, increased specific strength, increased specific modulus, increased thermal conductivity and increased wear resistance [9,10].

In the context of an armor application, composite armors have been made with ceramic strike faces (e.g., B_4C , SiC , Al_2O_3) and fiber-reinforced composites (e.g., Kevlar, Spectra), as they are effective at absorbing the kinetic energy of the projectile [11-13]. However, their high cost and mass have prompted research in finding alternative solutions. As such, researchers have begun to explore fabrication techniques for realizing cellular MMCs.

MMCs are fabricated through both solid state (e.g., powder metallurgy, diffusion bonding of foils) and liquid state (e.g., spraying, stir casting, squeeze casting into ceramic preforms, & electroforming) methods. Existing MMC techniques, such as infiltrating ceramic preforms made through press forming or foaming techniques, inherently limit the types of geometries that can be fabricated, and thus limit their application. As such, Garcia-Avila and co-authors created a composite armor [14] through a novel processing technique that forms a composite metal foam (CMF). This CMF is composed of hollow metallic spheres embedded in a solid metal matrix that is processed through powder metallurgy [15] and gravity casting techniques [16]. The resulting lightweight foam demonstrated the ability to absorb 60-70% of the total kinetic energy of a projectile and stopped both types of projectiles tested. However, one limitation of the processing technique is that it results in stochastic cellular topologies, and offers the designers little control over cell location, cell topology, and process repeatability.

1.3. Additive Manufacturing of Metal Matrix Composites

In an effort to provide a designer with control over the location of both cellular topology and the location of the encapsulated ceramic, the authors look to Additive Manufacturing (AM) as a means of realizing cellular MMCs. The layerwise fabrication approach of AM processes removes the geometric limitations often imposed by traditional manufacturing processes, and thus provides a designer with the freedom to effectively design the cellular mesostructure to maximize structural performance [17]. Binder Jetting [18], Selective Laser Melting [19,20], Electron Beam Melting [21,22], and Direct-Metal Laser Sintering [23] have all been employed in research targeted towards fabricating metallic cellular materials.

In addition, in an effort to provide the material property advantages of MMCs across a wider range of geometries, researchers are beginning to investigate the use of AM techniques as a means of processing MMCs. Much of the effort has been focused in powder metallurgy approaches wherein a metal/ceramic powder blend is processed either by powder bed fusion or

binder jetting AM techniques. Components fabricated from WC-Co [24,25], Fe & graphite [26], Ti & SiC [27], AlSiMg [28], and Fe & SiC [29] have been processed via AM. Sheet lamination AM techniques (e.g., ultrasonic consolidation) have also been used to produce fiber-reinforced MMCs [30,31]. There are a number of comprehensive reviews of AM of composite materials [32,33].

While these AM techniques have successfully produced MMCs with complex topologies, powder-based approaches are limited in that they are only able to produce parts with homogenous distribution of the composite material, and do not allow a designer to specify the location of ceramic material. In addition, the act of embedding a large foreign object (e.g., a premade tile for encapsulation) into a printed part is extraordinarily difficult (if not impossible) through powder bed techniques. While powder bed fusion AM processes have been successfully used to fabricate parts with cellular geometries, their ability to make parts of designed mesostructure is limited by inherent process constraints [34]. For example, support structures or anchors are often needed to combat the residual stresses imposed by rapid cooling of a melt; these structure must be manually removed in post-process, and can thus impose constraints on printable geometries. In addition, these processes have high cost, low throughput, and part size is limited by the dimensions of the build box.

1.4. Research Goal

In this work, the authors' goal is to create a cellular MMC fabrication approach that provides a designer control over the mesostructure topology of the metal cellular structure while also allowing for the embedding of ceramic materials to achieve MMC behavior [35]. Specifically, the authors present a manufacturing process chain in which binder jetting is used to print sand molds and cores for metal casting. These cores include pre-designed voids for receiving premade ceramic tiles for encapsulation during the casting operation, Figure 1.

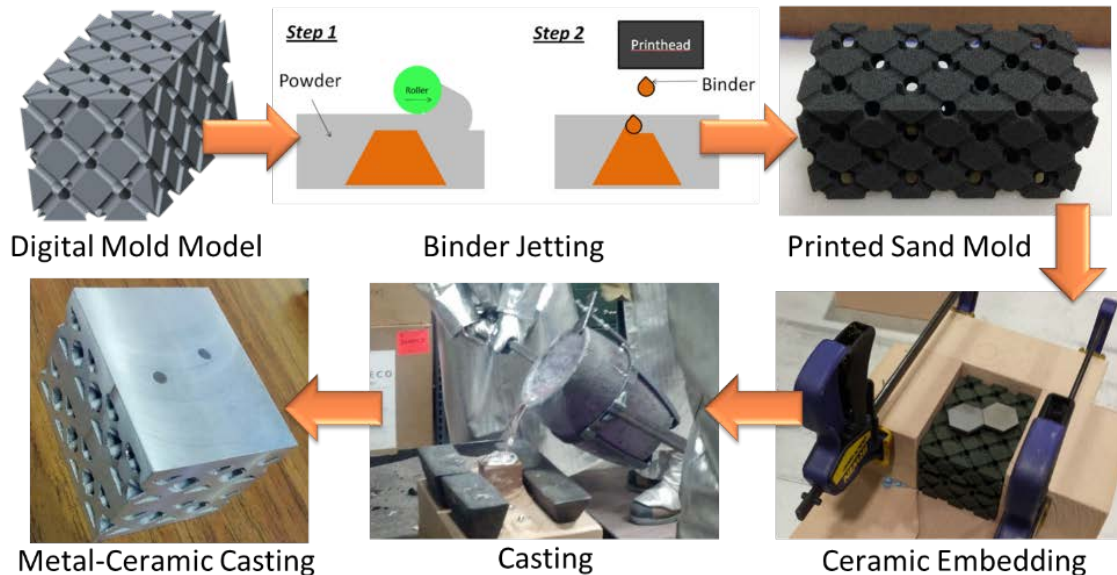


Figure 1. Overall process chain for realizing cellular MMCs via Binder Jetting AM, ceramic tile embedding, and metal casting.

By integrating ceramics into the printed sand molds, metal can be cast into the molds in order to create MMC lattice structures. This approach advances the state-of-the-art by creating lightweight metal-ceramic cellular composites with designed mesostructure, which is not able to be done with existing manufacturing technologies. Such a process would be able to produce artifacts composed of cast metallic trusses that can be designed to dissipate blast energy efficiently and high-density encapsulated ceramic or hard metal tiles that protect against penetration.

The overall goal of this work is to explore material compatibility and process feasibility for a variety of ceramic-metal combinations. An overview of the use of Binder Jetting AM to produce molds for casting lattice structures is presented in Section 2, along with a description of considerations of encapsulating ceramics with cast metal. Experimental methods for evaluating process feasibility and material compatibility are presented in Section 3. Results from these tests are presented in Section 4; closure is offered in Section 5.

2. Metal Casting of Metal-Ceramic Lattice Structures via Additive Manufacturing

2.1. Binder Jetting of Sand Molds

In casting applications, Binder Jetting AM artifacts are created through selective jetting of binder onto a powder bed of foundry sand. Once a layer has been printed, the powder feed piston rises, the build piston lowers, and a counter-rotating roller spreads a new layer of powder on top of the previous layer. The subsequent layer is then printed and is stitched to the previous layer by the jetted binder. Once the print is complete, the resulting mold is then depowdered and prepared for casting.

In their prior work, the authors demonstrated the effective use of binder jetting and metal casting to realize cast lattice structures [36]. The process begins with the digital design of the casting mold. As seen in Figure 2, the desired mesostructure is first modeled as a unit cell in CAD and then arrayed to create a repeating lattice structure. A Boolean subtraction of the mesostructure from the desired overall geometric shape provides a digital model of the casting mold, which is then sent to the binder jetting system.

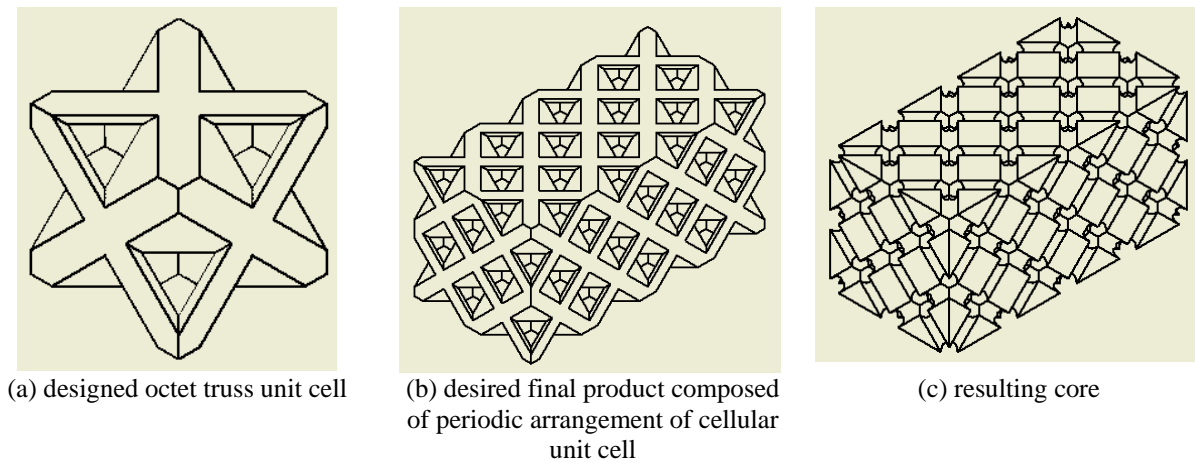


Figure 2. Digital design of cellular topology, lattice structure, and casting core.

This process provides the designer control over cellular topology and provides a scalable means of efficiently fabricating large cellular structures, Figure 3. Through finite element analysis of the energy absorption capabilities of an octet truss cellular structure created with the developed process, it was found that the cellular structure absorbed considerably more impact energy over that absorbed by a solid structure of the same mass [36].



Figure 3. Cast lattice structure resulting from a 3D printed sand mold.

Subsequent research has shown that the material properties of castings resulting from printed sand molds are nearly equivalent to those of traditional sand casting approaches [37]. In addition, manufacturing constraints of the sand printing process have also been evaluated to educate designers using the process [38].

2.2. Challenges in Casting Cellular Structures and Encapsulating Ceramic Tiles

This paper explores a two-part design that is comprised of a cast metallic truss structure that will dissipate blast energy efficiently and high-density encapsulated ceramic or white cast iron tiles that protect against penetration [39]. Manufacturing methods are challenging due to the different properties of materials used to create the composite component, including different melting points, different coefficients of thermal expansion, etc. Differing properties can lead to the formation of cracks and/or casting defects as the composite component cools (such as ceramic tile cracking due to thermal shock when contacted with the molten metal), which detract from the performance of the structure [40].

Areas of concern regarding the ceramic (boron carbide & aluminum oxide) and white cast iron tile encapsulations include wetting, thermal shock (tile cracking), and hot tearing (encapsulation cracking). Thermal shock can occur in ceramic materials when immersed in molten metals due to the thermal expansion difference between the surface in contact with hot metal and the interior [41]. Thermal shock is encouraged when the thermal conductivity of the material is low relative to the coefficient of thermal expansion. For this study, boron carbide & white cast iron (excellent thermal shock resistance) and aluminum oxide (poor thermal shock resistance) were examined (Section 3). Hot tears can occur on the surface of the metal encapsulation. A hot tear is a crack or irregularly-shaped fracture formed in a casting prior to completion of metal solidification because of hindered contraction and the resulting residual stresses. Hot tears are linked to inadequate compensation of solidification shrinkage by melt

flow in the presence of thermal stresses and are commonly associated with design limitations [42]. The tile encapsulations are particularly susceptible to hot tearing because of sharp edges and large thermal gradients.

Cast mesostructures can be a challenge to fill completely at reasonable pouring temperatures since the rod-shaped trusses have high diameter to length ratios (i.e., high surface area), which is a desirable design for the dissipation of energy in service, but an undesirable design for mold filling. The high surface area of the cast structure increases heat dissipation, which causes the metal to cool rapidly and potentially freeze before the mold is completely filled. This can result in an incomplete fill or porosity in the center of the structure [39]. There is an additional concern in filling molded mesostructures with embedded tiles; the tiles act as chills. The ceramic or white cast iron tiles rapidly remove heat from the molten metal, causing the metal to cool quickly and potentially freeze before completely encapsulating the tiles and/or filling the mesostructure.

3. Experimental Procedures

To test material compatibility and to evaluate the concerns noted in Section 2, the mesostructure and encapsulations were first tested individually. The two components were then combined into a metal-ceramic composite mesostructure with encapsulated tiles.

Previous research showed that it was possible to incorporate ceramic tiles into a cast aluminum mesostructure. In the previous research, encapsulation testing and cast mesostructure production was performed exclusively with an aluminum copper alloy and boron carbide tiles [39]. The current research included encapsulation testing of additional tile materials and geometries and cast mesostructure production using three additional metal alloys that had increasing melt temperatures and improved mechanical properties. Tables 1 & 2 show the cast metal plus tile combinations investigated and the cast metal alloys investigated with information on pouring temperature, tensile strength, and percent elongation to failure for each alloy. The iron-manganese-aluminum alloy (FeMnAl) had the best properties for this application, as well as the highest pouring temperature.

Table 1. Cast metal/tile combinations investigated.

<i>Metal Alloy</i>	<i>Tile Material & Geometry</i>
Al-Cu	boron carbide hexes, aluminum oxide rectangles, white cast iron hexes
Al-Si	boron carbide hexes, aluminum oxide rectangles, white cast iron hexes
FeMnAl	boron carbide hexes, aluminum oxide rectangles, white cast iron hexes

Table 2. Metal alloys investigated [39,43-45].

<i>Metal Alloy</i>	<i>Typical Pouring Temperature</i>	<i>Ultimate Tensile Strength</i>	<i>Elongation to Failure</i>
Al-Cu	730°C	420 MPa	6%
C95800 Nickel-Aluminum-Bronze	1277°C	580 MPa	18%
HY-80 Steel	1593°C	690 MPa	20%
FeMnAl	1650°C	up to 2 GPa reported	up to 70% reported

Mesostructures were produced using alloys with increasingly high pouring temperatures (noted in Table 2), including an aluminum copper alloy, nickel-aluminum-bronze, HY-80 steel, and FeMnAl. The mesostructure castings were 150mm x 150mm by 115 or 165mm tall (6"x6" by 4.5 or 6.5" tall), had 5mm (0.2") diameter trusses, 6.35mm (0.25") thick face sheets and had 63% open volume. 3D printed mold "cores" and sleeves were used for production of mesostructures with and without encapsulations, as well as for production of just encapsulated tiles. A 3-D printed core and sleeve used for casting mesostructures is shown in Figure 4. The molds were designed to bottom fill to reduce turbulence and two downsprues were used to reduce temperature loss during mold filling.

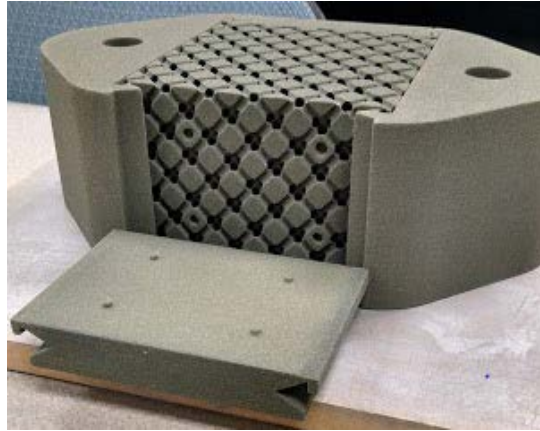


Figure 4. 3D printed core and sleeve for cast mesostructure production.

As seen in Figure 5, the mold package featured pre-designed voids to accommodate the embedding of ceramic tiles. Locating pins were placed inside the voids to position the ceramic tiles during the mold assembly process and to hold them in place during the pour.

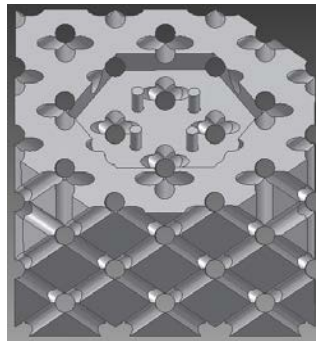


Figure 5. CAD model of the mold mesostructure featuring void and locating pins for ceramic tile encapsulation.

ProCast software was used to simulate mold filling and solidification. The modeling software indicated that filling was somewhat turbulent at the beginning due to two metal fronts coming together, Figure 6a, but shortly thereafter became quite uniform with very little turbulence as indicated by a planar metal front moving up the casting, Figure 6b. Solidification analysis indicated that porosity may be present in the middle of the casting since this was the last area to solidify and was isolated, Figure 7.

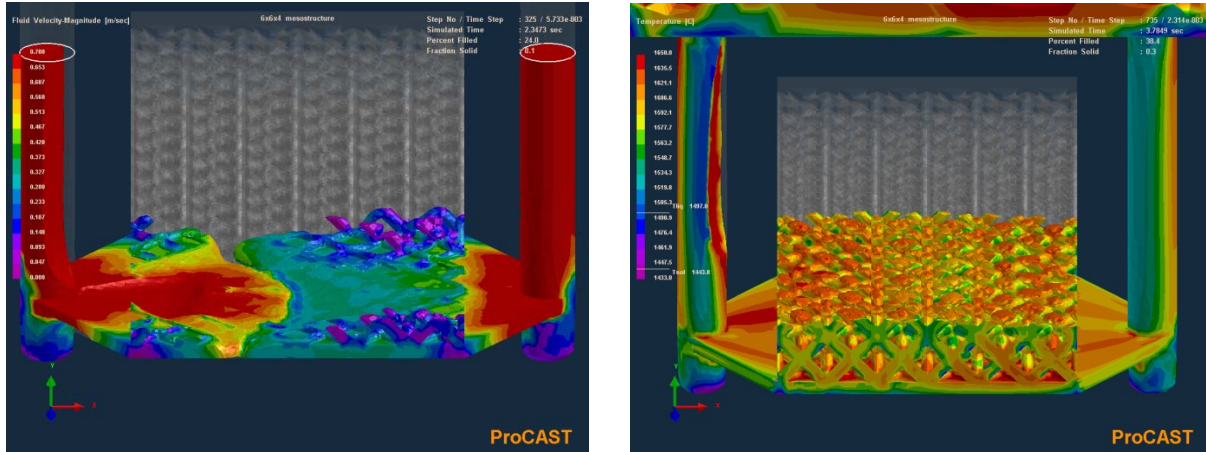


Figure 6. (a) Mold filling analysis showing turbulent filling conditions as the two metal fronts come together. (b) Mold filling analysis showing quiet, uniform fill shortly after the two metal fronts come together.

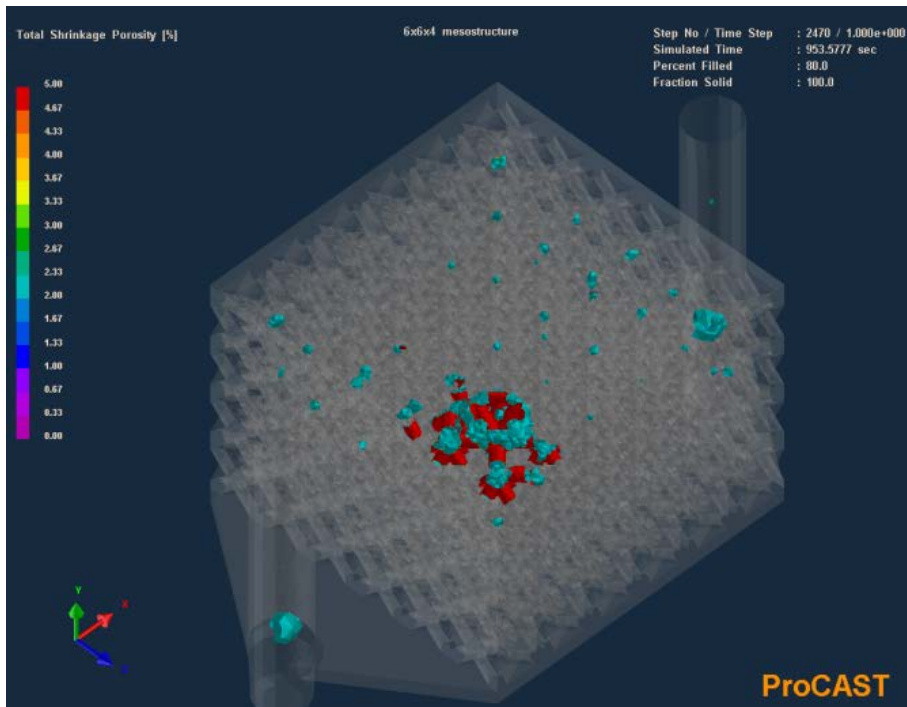


Figure 7. Solidification analysis showing the potential for porosity in the middle of the casting.

Aluminum oxide tiles (6.35mm, 0.25” thick), boron carbide tiles (4mm, 0.16” & 9mm, 0.35” thick), and white cast iron tiles (4mm, 0.16” & 9mm, 0.35” thick) were encapsulated in Al-Si, Al-Cu, and FeMnAl alloys. Three different encapsulation thicknesses were evaluated: 3.2mm (0.125”), 4.8mm (0.188”) and 6.35mm (0.250”). The design evolution of the sand molds for encapsulation studies are shown in Figure 8. X-ray analysis was performed on the finished encapsulations to check for cracked or shattered tiles.

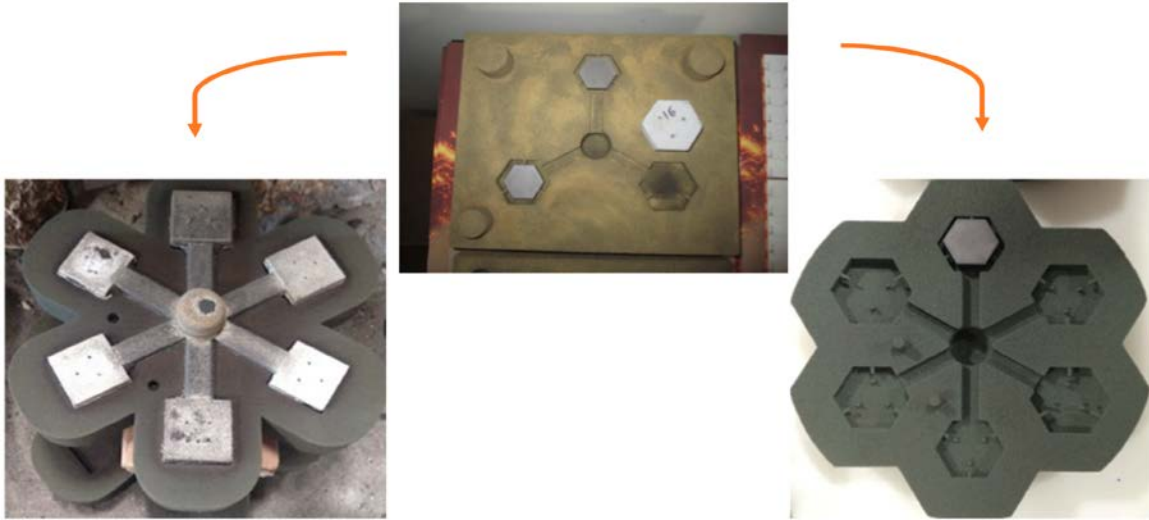
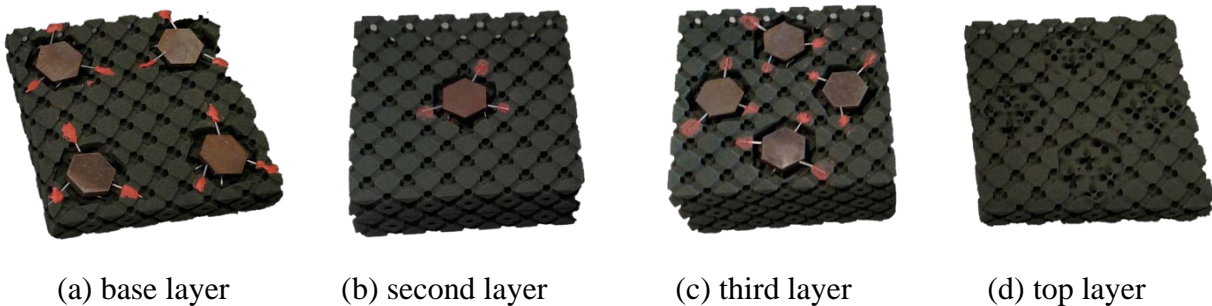


Figure 8. 3D printed sand encapsulation molds showing the design evolution.

In addition, a 150x150x115mm FeMnAl composite lattice structure with encapsulated white cast iron tiles was produced. The printed sand mold had four “core” layers, with space for tiles to be placed into each layer, as shown in Figure 9. The tiles were arranged in a high-density configuration in order to insure that a projectile would hit at least one tile. The tiles were held in place for pouring with aluminum wire attached to the mold with core paste. The “core” layers were stacked and placed in a 3D printed sand sleeve. A pouring basin made from conventional bonded sand was placed on top of the assembled sleeve. High temperature, zirconia filters were used to insure clean metal and thin steel sheet covered the downsprues to insure that the pouring basin would be partially full of metal before mold filling occurred to prevent the possibility of an interrupted pour.



(a) base layer

(b) second layer

(c) third layer

(d) top layer

Figure 9. Layered 3D printed “core” molds for a mesostructure with encapsulations.

4. Results and Discussion

Visual and X-ray analysis showed that all encapsulations in Al-Si alloy were successful with no hot tearing or cracked tiles, Figure 10. Tiles encapsulated in Al-Cu alloy showed mixed results. Figure 11a shows a white cast iron tile encapsulated in Al-Cu alloy that exhibited hot tearing and Figure 11b shows an aluminum oxide tile encapsulated in Al-Cu alloy that exhibited lack of complete encapsulation and tile cracking.

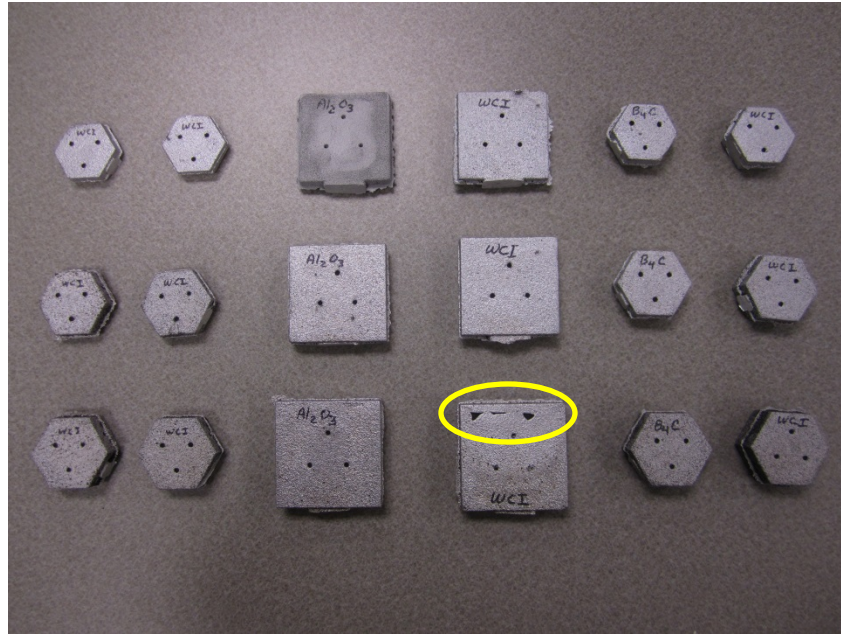


Figure 10. Examples of tiles encapsulated in Al-Si alloy that exhibited no defects except for one white cast iron tile that moved out of position and tilted during pouring.



(a) White cast iron tile encapsulated in Al-Cu alloy exhibiting hot tearing



(b) Al_2O_3 tile encapsulated in Al-Cu alloy exhibiting lack of complete encapsulation and tile cracking

Figure 11. Examples of tiles encapsulated in Al-Cu alloy that exhibited defects.

Encapsulation in FeMnAl was partially successful. Boron carbide tiles were either successfully encapsulated or exhibited cracking due to thermal shock. White cast iron tiles were either successfully encapsulated or exhibited hot tearing of the encapsulant, and aluminum oxide tiles all fractured due to thermal shock. Examples of successful and unsuccessful encapsulations in FeMnAl are shown in Figure 12. The white cast iron tiles encapsulated in FeMnAl showed porosity and no bonding at the encapsulant/tile interface, Figure 13.

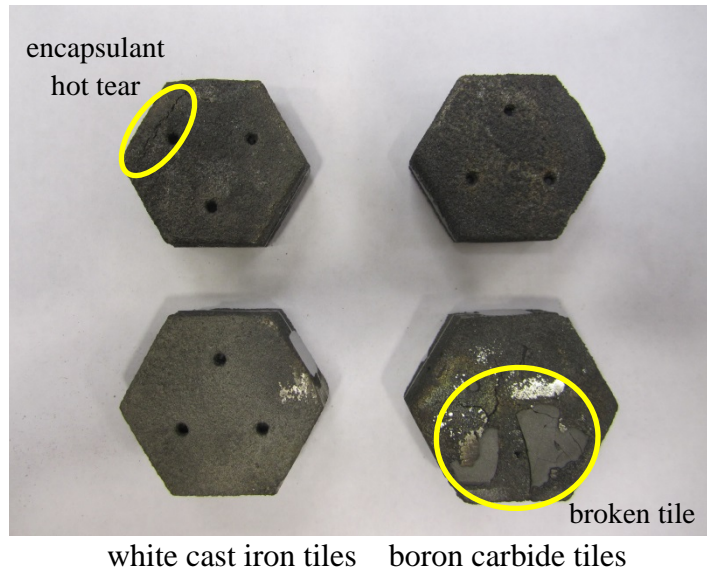


Figure 12. Examples (good & bad) of tiles encapsulated in FeMnAl.

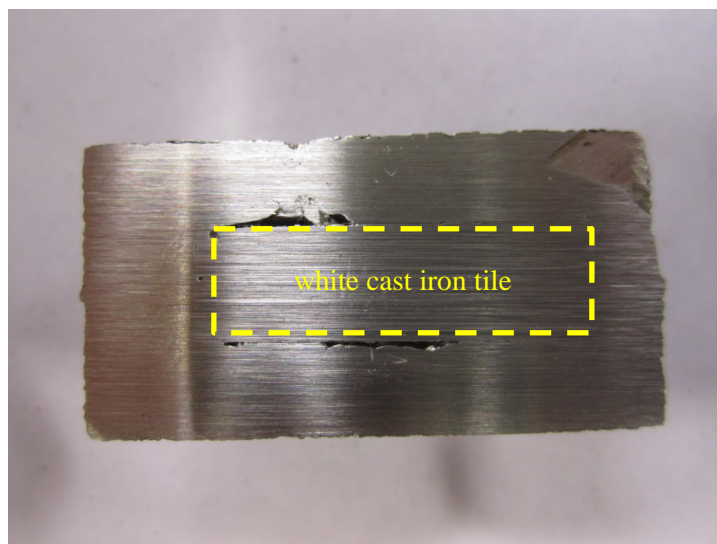


Figure 13. Porosity and lack of bonding at the interface between FeMnAl encapsulant and white cast iron tile.

Mesostructures were successfully cast from aluminum-copper alloy, nickel-aluminum-bronze, HY-80 Steel, and FeMnAl. Each casting exhibited complete fill based on visual analysis, Figure 14. As noted previously, solidification modeling indicated that porosity may be present in the center of the casting due to shrinkage caused by the lack of risers/feeders. The porosity could not be examined visually, so it is undetermined if there is any porosity or shrinkage in the center of these castings. X-ray analysis (preferably X-ray computed tomography) could be used to quantify internal defects.

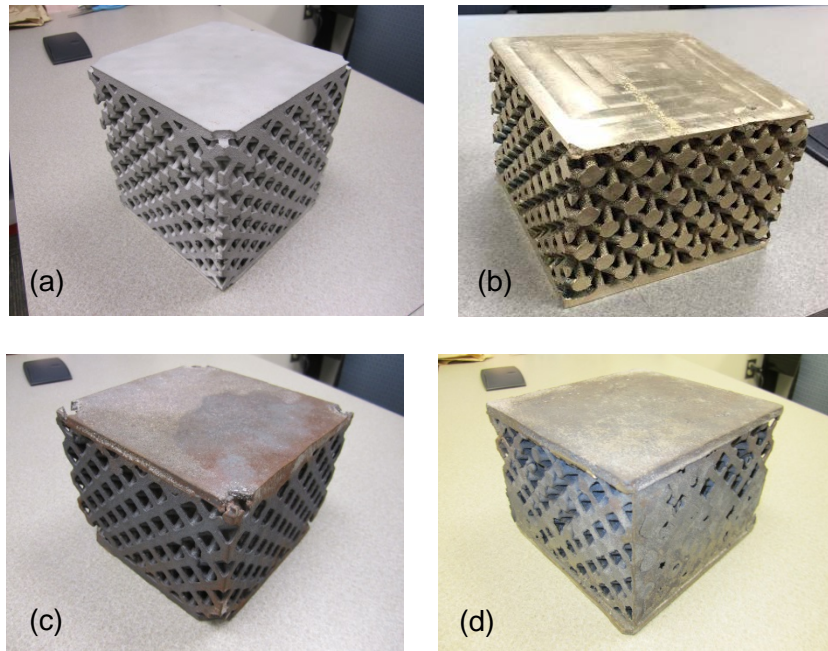


Figure 14. (a) aluminum-copper alloy, (b) nickel-aluminum-bronze, (c) HY 80 steel and (d) FeMnAl mesostructure castings showing complete fill.

Of the two cast metal-ceramic composite mesostructures constructed of FeMnAl and white cast iron tiles, one was successful, and the other failed to completely fill. The FeMnAl chemistry for these mesostructures with encapsulations was 31 wt% Mn, 4.2 wt% Al, 0.8 wt% Si, 0.9 wt% C, 0.5 wt% Mo. The successful FeMnAl structure was poured at 1675°C (3050°F), and the structure that did not fill was poured at 1620°C (2950°F). Since the failed structure was poured at a lower temperature, the molten metal cooled and froze too quickly. The resulting castings are shown in Figure 15.



(a) Successful casting poured at 1675°C.



(b) Unsuccessful casting poured at 1620°F.

Figure 15. FeMnAl mesostructure castings with encapsulated white cast iron tiles.

5. Conclusions and Future Work

1. Complex, lightweight, mesostructure castings with or without encapsulated tiles can be produced in non-ferrous and ferrous metals using 3D printed sand molding technology.
2. Ceramic and metallic tiles can be encapsulated in non-ferrous and ferrous metals using 3D printed sand molding technology. Aluminum oxide, boron carbide and white cast iron tiles can be successfully encapsulated in aluminum alloys and boron carbide and white cast iron tiles can be successfully encapsulated in FeMnAl alloy. At present, no bonding has been observed between the encapsulant and the ceramic or metallic tiles.
3. Complex mesostructure castings can be produced by casting facilities using gravity pouring; special or unique casting processes are not required.

Optimization of the lattice geometry to facilitate incorporation of tiles, and allow casting of wider and thinner structures would be valuable future additions to this research. Exploration of additional metal-ceramic material combinations for encapsulations, optimization of FeMnAl production methods, and mechanical/physical testing (including ballistic testing) of the cast structures would provide direction for improving the energy dissipation properties, blast tolerance and penetration resistance of these cast structures.

6. Acknowledgments

The authors would like to acknowledge the Virginia Tech graduate and undergraduate students that have contributed to this research effort over the past five years: Drs. Drew Snelling & Nick Meisel began this project and developed a long term research strategy, Q. Li performed blast modeling, Erin Connelly performed ProCast analysis, and the undergraduate senior design team of Allison Popernack, Avalon Schuler, Ian Knudsen and Matt Antonelli, and the undergraduate senior design team of Heather Blount, Charles Forman, Kelly Ramsburg and Andrew Wentzel generated valuable research data. The authors express their sincere thanks to ExOne for providing the 3D printed sand molds & cores and for numerous discussions on efficient 3D printed sand mold design. The authors also wish to thank the DREAMS (Design, Research and Education for Additive Manufacturing Systems) Lab graduate students, particularly Dr. Drew Snelling, for assistance in the development of the mesostructure design and the VT-FIRE (Virginia Tech Foundry Institute for Research and Education) graduate students for assistance in molding, melting, molten metal treatment and pouring of these castings at the Virginia Tech Kroehling Advanced Materials Foundry. Precision Castparts Corporation, Airfoils LLC performed the X-ray analysis of the encapsulated tiles.

This material is based upon work supported by the National Science Foundation under Grant No. 1462089. Any opinions, findings, and conclusions or recommendations expressed in this material are those of the author(s) and do not necessarily reflect the views of the National Science Foundation.

7. References

1. Gibson, J. W., and Ashby, M. F., 1997, *Cellular Solids: Structures and Properties*, Cambridge University Press, Cambridge, UK.
2. Banhart, J., 2000, "Manufacturing Routes for Metallic Foams," *Memb. J. Miner. Met. Mater. Soc.*, 52 (December).
3. Degischer, H.-P., and Kriszt, B., 2002, *Handbook of Cellular Metals: Production, Processing, Applications*.
4. Thompson, S. C., Muchnick, H., Choi, H., and McDowell, D., 2006, "Robust Materials Design of Blast Resistant Panels," *Multidisciplinary Analysis and Optimization Conference*, pp. 1–15.
5. Banhart, J. and D. Weaire, 2002, "On the Road Again: Metal Foams Find Favor," *Physics Today*, July, pp. 37-42.
6. Wadley, H. N. G., N. A. Fleck and A. Evans, 2003, "Fabrication and Structural Performance of Periodic Cellular Metal Sandwich Structures," *Composites Science and Technology*, Vol. 63, pp. 2331-2343.
7. Clyne, T. W., and Withers, P. J., 1993, *An Introduction to Metal Matrix Composites*, Cambridge University Press.
8. Schleg, Frederick P. "Technology of Metalcasting." American Foundry Society, 2003, p.111.
9. Suresh, S., Mortensen, A., and Needleman, A., 1993, *Fundamentals of Metal-Matrix Composites*, Butterworth-Heinemann, Boston.
10. Hunt, W.H., Herling, D.R., "Aluminum Metal Matrix Composites," *Advanced Materials & Processes*, February 2004, pp.39-42.
11. Medvedovski E. Ballistic performance of armour ceramics: Influence of design and structure. Part 1. *Ceram Int* 2010;36:2103–15.
12. Medvedovski E. Ballistic performance of armour ceramics: Influence of design and structure. Part 2. *Ceram Int* 2010;36:2117–27.
13. Medvedovski E. Lightweight ceramic composite armour system. *Adv Appl Ceram* 2006;105:241–5.
14. M. Garcia-Avilaa, M. Portanovab, A. Rabieia "Ballistic performance of composite metal foams," *Composite Structures*, Volume 125, July 2015, Pages 202–211.
15. Neville BP, Rabiei A. Composite metal foams processed through powder metallurgy. *Mater Des* 2008;29:388–96.
16. Vendra LJ, Rabiei A. A study on aluminum–steel composite metal foam processed by casting. *Mater Sci Eng A* 2007;465:59–67.
17. Evans, A. G., J. W. Hutchinson, N. A. Fleck, M. F. Ashby and H. N. G. Wadley, 2001, "The Topological Design of Multifunctional Cellular Metals," *Progress in Material Science*, Vol. 46, pp. 309-327.
18. C. B. Williams, J. K. Cochran, D. W. Rosen, 2011, "Additive Manufacturing of Metallic Cellular Materials via Three-Dimensional Printing," *The International Journal of Advanced Manufacturing Technology*, Vol. 53, No. 1-4, pp. 231-239 (DOI 10.1007/s00170-010-2812-2).
19. Pham, D. T., Dimov, C. J., and Gault, R. S., 2003, "Layer Manufacturing Processes: Technology Advances and Research Challenges," 1st International Conference on Advanced Research in Virtual and Rapid Prototyping, Leiria, Portugal, pp. 107–113.

20. Brooks, W., Sutcliffe, C., Cantwell, W., Fox, P., Todd, J., and Mines, R., 2005, "Rapid Design and Manufacture of Ultralight Cellular Materials," International Solid Freeform Fabrication Symposium, Austin, TX, pp. 231–241.
21. Cansizoglu, O., Cormier, D., Harrysson, O., West, H., and Mahale, T., 2006, "An Evaluation of Non-Stochastic Lattice Structures Fabricated Via Electron Beam Melting.," International Solid Freeform Fabrication Symposium, Austin, TX, pp. 209–219.
22. Yang, L., Harrysson, O., West II, H., and Cormier, D., 2011, "Design and characterization of orthotropic re-entrant auxetic structures made via EBM using Ti6Al4V and pure copper," International Solid Freeform Fabrication Symposium, Austin, TX, pp. 464–474.
23. Agarwala, M., Bourell, D., Beaman, J., Marcus, H., and Barlow, J., 1995, "Direct selective laser sintering of metals," *Rapid Prototyp. J.*, **1**(1), pp. 26–36.
24. Laoui T, Froyen L, Kruth JP. Effect of mechanical alloying on selective laser sintering of WC–9CO powder. *Powder Metal* 2000;42(3):203–5
25. Maeda K, Childs THC. Laser sintering (SLS) of hard metal powders for abrasion resistant coatings. *J Mater Process Technol* 2004;149(1–3):609–15
26. Simchi A, Pohl H. Direct laser sintering of iron–graphite powder mixture. *Mater Sci Eng A* 2004;383(2):191–200
27. Vaucher S, Paraschivescu D, Andre C, Beffort O. Selective laser sintering of aluminium–silicon carbide metal matrix composites. *Mater Week*; 2002.
28. Manfredi D, Calignano F, Krishnan M, Canali R, Ambrosio EP, Atzeni E. From Powders to Dense Metal Parts: Characterization of a Commercial AlSiMg Alloy Processed through Direct Metal Laser Sintering. *Materials*. 2013; 6 (3): 856-869
29. Ramesh CS, Srinivas CK, Channabasappa BH. Abrasive wear behaviour of laser-sintered iron–SiC composites. *Wear* 2009. doi:10.1016/j.wear2008.12.026.
30. Kong CY, Soar RC, Dickens PM. Ultrasonic consolidation for embedding SMA fibres within aluminium matrices. *Compos Struct* 2004;66(1–4):421.
31. Yang Y, Janaki Ram GD, Stucker BE. Bond formation and fiber embedment during ultrasonic consolidation. *J Mater Process Technol* 2009;209(10):4915–24.
32. S. Kumar and J.-P. Kruth, "Composites by rapid prototyping technology," *Materials and Design*, 31 (2010) 850–856.
33. D. Manfredi, F. Calignano, M. Krishnan, R. Canali, E. Paola Ambrosio, S. Biamino, D. Ugues, M. Pavese and P. Fino, "Additive Manufacturing of Al Alloys and Aluminium Matrix Composites (AMCs)," *Light Metal Alloys Applications*, ed. W. A. Monteur, DOI: 10.5772/58534.
34. C. B. Williams, F. Mistree, D. W. Rosen, 2005, "Investigation of Additive Manufacturing Processes for the Manufacture of Parts with Designed Mesostructure," ASME IDETC 10th Design for Manufacturing and the Life Cycle Conference, September 24-28, Long Beach, CA, Paper No. DETC2005/DFMLC-84832.
35. D. Snelling, C. B. Williams, C. Suichital, A. Druschitz, 2015, "Fabrication of Cordierite Preforms via Binder Jetting," International Solid Freeform Fabrication Symposium, Austin, TX.
36. D. Snelling, Q. Li, N. Meisel, C. B. Williams, R. C. Batra, and A. P. Druschitz, "Lightweight Metal Cellular Structures Fabricated via 3D Printing of Sand Cast Molds," *Advanced Engineering Materials*, published online March 11, 2015 (DOI: 10.1002/adem.201400524).

37. D. Snelling, H. Blount, C. Forman, K. Ramsburg, A. Wentzel, C. B. Williams, A. Druschitz, 2013, "3D Printed Molds and Their Effects on Metal Castings," International Solid Freeform Fabrication Symposium, Austin, TX.
38. D. Snelling, C. B. Williams, A. Druschitz, 2014, "Complex Geometrical Effects on Depowdering and Solidification in Sand Molds Fabricated via Binder Jetting," International Solid Freeform Fabrication Symposium, Austin, TX.
39. Popernack, Allison. "Cast Aluminum Mesostructures Using 3D Printed Sand Cores with an Encapsulation." *International Journal of Metalcasting*, vol. 10, pp.111-113, Jan. 2016.
40. Tenold, Tyrus N. "Ballistic Applications of Composite Materials." Spokane Industries, assignee. Patent US0240755A1, Sept. 27, 2012.
41. M. Fellner and P. Supancic, "Thermal shock failure of brittle materials," *Fractography of Advanced Ceramics*, vol. 223, pp. 97-106, 2002.
42. Schleg, Frederick P. "Technology of Metalcasting." American Foundry Society, pp. 328, 2003.
43. Richardson, I., "Guide to Nickel Aluminum Bronze for Engineers," edited by C. Powell, Copper Development Association Publication No. 222, Jan. 2016.
44. Arpin, K.R., Trimble, T.F., "Material Properties Test to Determine Ultimate Strain and Stress-True Strain Curves for High Yield Steels." General Dynamics, Report No. TDA-19194, April 2003.
45. Howell, R., "Microstructural Influence on Dynamic Properties of Age Hardenable FeMnAl Alloys." Army Research Lab, April 2011.